





Artificial Neural Network Models for Predicting Required Cross-section Dimensions of Concrete Filled Steel Tubular Columns



Samir Al-Zgul¹ , Vasilina Tyurina¹ , Anton Chepurnenko^{1,*}  and Vladimir Akopyan² 

¹ Structural Mechanics and Theory of Structures Department, Don State Technical University, Rostov-on-Don, Russia

² Bases and Foundations Department, Don State Technical University, Engineering Geology, Rostov-on-Don, Russia

Abstract:

Background: Artificial Neural Networks (ANN) can be a useful tool to assist in the design of reinforced concrete structures. The aim of this paper is to develop artificial neural network models for predicting the required diameter of eccentrically compressed concrete-filled steel tubular (CFST) columns and the wall thickness of the steel pipe.

Methods: Within the framework of the set goal, three models of ANN were developed. The first model predicts the required cross-sectional diameter for the minimum pipe wall thickness. The second model solves the same problem for the maximum possible wall thickness. The input parameters of the first two models are the axial force, bending moment, strength characteristics of steel and concrete, column length, and a coefficient characterizing the share of constant and long-term loads in the total load. The third model predicts the required wall thickness based on the listed parameters, as well as the column diameter. Synthetic data, including more than 2 million samples, was generated to train the models. The ANN architecture is a feedforward neural network with 2 hidden layers containing 16 neurons each. Machine learning models are implemented in the MATLAB environment.

Results: The trained models showed high performance in terms of mean squared error and correlation coefficient between the target and predicted values of the output parameter. The importance of features was also assessed using the variable fixation method. It has been established that the required value of the column diameter is most significantly influenced by the magnitude of the bending moment, axial force and column length. The required pipe wall thickness is most influenced by the magnitude of internal forces and the diameter of the column.

Conclusion: The developed models of artificial neural networks are an effective and reliable tool that can help a civil engineer in the design of buildings and structures that include CFST elements.

Keywords: Concrete-filled steel tubular columns, Artificial neural network, Feature importance, Inverse problem, Mean squared error, Bearing capacity.

© 2025 The Author(s). Published by Bentham Open.

This is an open access article distributed under the terms of the Creative Commons Attribution 4.0 International Public License (CC-BY 4.0), a copy of which is available at: <https://creativecommons.org/licenses/by/4.0/legalcode>. This license permits unrestricted use, distribution, and reproduction in any medium, provided the original author and source are credited.

* Address correspondence to this author at the Structural Mechanics and Theory of Structures Department, Don State Technical University, Rostov-on-Don, Russia; E-mail: anton_chepurnenk@mail.ru

Cite as: Al-Zgul S, Tyurina V, Chepurnenko A, Akopyan V. Artificial Neural Network Models for Predicting Required Cross-section Dimensions of Concrete Filled Steel Tubular Columns. Open Civ Eng J, 2025; 19: e18741495387193. <http://dx.doi.org/10.2174/0118741495387193250411105201>



CrossMark

Received: January 20, 2025

Revised: February 08, 2025

Accepted: March 06, 2025

Published: April 21, 2025



Send Orders for Reprints to
reprints@benthamscience.net

1. INTRODUCTION

In conditions of limited urban space, modern construction tends to increase the height of buildings and floor spans, which dictates the need to use columns with high load-bearing capacity. One of the promising solutions

to this problem is concrete-filled steel tubular (CFST) structures, which provide an optimal combination of strength and functionality. Circular CFST columns have high axial compressive strength [1], which is their main advantage and allows them to be widely used in modern construction, including high-rise buildings, long-span

bridges, underground tunnels and unique infrastructure facilities [2-4].

The ability to maintain structural integrity and stability in emergency situations is of key importance for CFST structures due to the ability to effectively absorb significant amounts of energy during deformation [5, 6]. In addition, such structures help reduce the impact on the environment due to the rejection of the traditional formwork use, recycling of steel pipes and the use of high-quality concrete with recycled aggregate [7].

Research conducted in the field of improving the calculation of CFST columns can be divided into several categories: full-scale experiments, calculations performed in accordance with national design standards (Eurocode4, AISC 360-16, SR 266.1325800.2016, *etc.*), numerical calculations in finite element software packages (ABAQUS, ANSYS, *etc.*) [8], artificial intelligence (AI) technologies and research that combine the above methods.

Laboratory experimental studies have traditionally been used to analyze the behavior of CFST columns, but their application is limited by a narrow parameter range, high cost, and significant labor costs. Kloppel and Gorder [9] conducted the first experimental studies of CFST columns in the 1950s. Since then, many experimental studies have been conducted to analyze the structural behavior of CFST columns [10-15]. The geometric and physical-mechanical data obtained from these and other experimental studies are actively used to train and test artificial intelligence models aimed at predicting the design results of CFST columns. AI models provide a better fit to experimental data and increased adaptability, overcoming the limitations of traditional nonlinear or analytical models [16].

Over the past 10 years, there has been an exponential growth in publications on CFST calculation using machine learning (ML) technologies. It can be confirmed by a search carried out in the Google Scholar scientometric database by keywords "CFST" and "Machine Learning."

Numerous studies have demonstrated the effectiveness of ANNs (artificial neural networks) technology in solving complex problems in the field of CFST calculation.

Thus, the authors of papers [17, 18] investigated the prediction of the bearing capacity for short CFST columns under axial load using ANN based on a large amount of experimental data. Comparative analysis of ANN and the empirical regression model revealed a clear advantage of ANN. R^2 (the coefficient of determination) was 0.97 for ANN versus 0.926 for the regression model, and MAPE (mean absolute percentage error) reached 5.8% for ANN and 13.2% for the regression model. The study demonstrated that the use of ANN allows for achieving greater accuracy in predicting the bearing capacity of CFST columns compared to the previously proposed empirical regression model. Du *et al.* [19]. also used ANN technology for rectangular columns with good results. The mean value of output parameters μ was equal to 1.013, which shows a small deviation from the expected value.

The coefficient of variation CoV was equal to 0.0702, which indicates good stability of the model. These metrics indicate that the neural network model has stable predictions with a small deviation from the mean.

Le *et al.* [20]. used Gaussian process regression (GPR) to predict the ultimate bearing capacity of rectangular CFST columns. As shown in this study, this method provides high prediction accuracy for the following metrics: $R^2 = 0.9956$, RMSE = 154.66 (root mean square error), MAPE = 7.54%, the values of which indicate high agreement between the predicted and experimental values.

Tran's works [21-23] present approaches to predicting the strength of columns using ANN models and a polynomial regression model. In a study [23], ANN demonstrated high prediction accuracy: $\mu=1.05$, CoV = 0.07, $R^2 = 0.996$, a20-index = 0.993 (accuracy index) and MSE = 0.011535. These indicators confirm the minimal variation and almost perfect correspondence of the model predictions to the actual data. At the same time, the polynomial regression model [21] showed the following metrics: MAPE = 22%, MAE = 559.7 (mean absolute error), RMSE = 789.8, $R^2 = 0.98$, $\mu = 1.18$, CoV = 0.25. Although the coefficient of determination remains high, the error and variance values indicate that this model is less accurate than ANN.

The model based on genetic programming (GEP) for circular CFST columns presented in a study [24] demonstrates high prediction accuracy. The MAPE value of 7.49% indicates a small relative error, which is a good result for engineering calculations; the low RMSE value of 228 confirms that the model provides minimal deviations between predicted and actual values. These indicators show that the GEP method can be effectively used to predict the strength of columns with a high degree of reliability.

In a study [25], a model for calculating circular CFST column based on GEP is presented, which demonstrated the following accuracy metrics: RMSE = 258, $R^2 = 0.98$, MAE = 138.7, $\mu = 1.2$, and CoV = 0.1. These metrics indicate the high accuracy of the model: a small RMSE and low MAE indicate minimal deviations between actual and predicted values. The determination coefficient shows that the model explains 98% of the data variation, which confirms its reliability. The μ and CoV values indicate good stability and predictability of the model. Overall, GEP [25] has proven itself to be an effective method for forecasting with a high degree of accuracy and reliability.

Hybrid methods such as genetic algorithm (GA) and GEP were used to analyze columns of different shapes [26]. These methods achieved high results, with a determination coefficient of 0.98 and a variation coefficient within 13%-15%. These results indicate high accuracy and stability of the forecast when using hybrid methods to evaluate column characteristics.

In another work [27], the author considers two prediction methods for circular columns: GEP and ANN, each of which demonstrated its own characteristics and advantages in assessing the strength of columns.

GEP showed the following results: $\mu = 0.98$ indicates high accuracy of the model, but with some variations in the data, which is confirmed by $\text{CoV} = 0.22$. The coefficient of determination (0.98) confirms its high accuracy. However, the values of $\text{MAE} = 242$ and $\text{RMSE} = 384$ show that this model may require further optimization to improve the accuracy of predictions. At the same time, ANN demonstrated higher indicators: $\mu = 0.99$ and $\text{CoV} = 0.13$, showing greater stability and accuracy of the model, with minimal deviations from the actual values, $R^2 = 0.99$ indicates an almost perfect match between the predictions and real data. The indicators $\text{MAE} = 134$ and $\text{RMSE} = 205$ confirm that the neural network more accurately predicts the strength of circular columns, providing significantly smaller errors compared to GEP.

In a study [28], the strength analysis of CFST columns was conducted using various machine learning models, including GPR-based regression, symbolic regression (SR), support vector regression (SVR), ANNs, extended gradient boosting (XGBoost), categorical optimized boosting (CatBoost), particle swarm optimized support vector regression (PSVR), random Forest and LightGBM. To test the accuracy and reliability of these approaches, the predictions obtained with their help were compared with the results calculated using national design codes.

The results of the study [28] demonstrated that the CatBoost, GPR, PSVR and XGBoost models showed the highest accuracy and reliability for estimating the strength of CFST columns. For example, when analyzing the strength of circular columns, the accuracy metrics confirm the superiority of these methods. The average prediction values for CatBoost, GPR and PSVR were close to one (1.0), indicating the high accuracy of the models. The coefficient of variation, which characterizes the stability of the model, was minimal for CatBoost and GPR (0.017 and 0.026, respectively), indicating the high reliability of their predictions. The determination coefficient (R^2) is close to 1, which confirms the exact match between the predicted and experimental data. The average absolute percentage error for CatBoost was only 0.711%, and the root mean square error was minimal (89.9). In addition, the a20 index (the proportion of forecasts with an error of less than 20%) for CatBoost and GPR reached its maximum value of 1.0.

The multi-objective optimization approach presented in the study [29] determines the optimal parameters for eccentrically loaded short CFST columns with circular cross-sections using linear regression models and genetic algorithms to optimize parameters such as diameter, thickness, and compressive strength while constraining the upper and lower bounds of these parameters in accordance with the international standards AISC 360-16 and Eurocode4. By minimizing the mean square error between the predicted and actual values, the optimization

platform developed in the MATLAB environment offers a tool for designing efficient and durable CFST columns, enhancing the overall reliability of structural design in the construction industry.

In studies of CFST column strength prediction, ANN, GEP, regression models, SVM, CatBoost, and GPR were used. ANN provides high accuracy ($R^2 > 0.95$), GEP allows flexible identification of analytical dependencies, regression models are easy to implement but limited in complex nonlinear dependencies, and SVM demonstrates efficiency when working with high-dimensional data and resistance to overfitting. CatBoost and GPR showed the highest accuracy, minimum average absolute percentage error, and high stability of forecasts, which makes them the most promising for engineering practice.

The conducted literature review shows that the aim of most studies is to determine the bearing capacity of CFST columns. For a civil engineer, an equally important task is to determine the required cross-section dimensions of columns when the values of internal forces are known. The solution to this problem is usually carried out by selection through a variety of options, which is a rather labor-intensive task and does not always lead to the most optimal result. Selection of the CFST columns cross-section dimensions using machine learning methods has not been performed before. The purpose of this paper is to develop artificial neural network models for predicting the required diameter of eccentrically compressed concrete-filled steel tubular (CFST) columns and the wall thickness of the steel pipe.

2. MATERIALS AND METHODS

The object of study in this article is eccentrically compressed concrete-filled steel tubular (CFST) columns without bar reinforcement inside the concrete core.

To solve the problem of selecting the cross-sectional dimensions of CFST columns, three models of artificial neural networks were developed. The input parameters of the first model are the following values:

1. Compressive axial force N , kN;
2. Bending moment M , kN · m ;
3. Yield strength of steel R_y , MPa;
4. Compressive strength of concrete R_b , MPa;
5. Design length of column l , m;
6. A coefficient φ_l that takes into account the influence of the load duration and is determined by the formula (a):

$$\varphi_l = 1 + \frac{M_{ll}}{M_1}, \quad (\text{a})$$

where M_l and M_{ll} are respectively bending moments from the action of the full load and from the action of constant and long-term loads.

The first model predicts the required value of the CFST column outer diameter D_{pi} with a minimum wall thickness of a steel pipe according to the Russian

assortment “GOST 10704-91. Electrically welded steel line-weld tubes. Range”. The second model has the same input parameters but, unlike the first model, predicts the required value of the outer diameter D_{p2} when the pipe wall thickness is maximum. When the pipe wall thickness takes the minimum possible value, the section diameter will be the maximum, but we will have the most economical design in terms of cost. When the pipe wall thickness takes the maximum possible value according to the assortment, the pipe diameter will be minimum. Such a design will have the highest cost, but it will be distinguished by its compactness.

When designing, a balance is often needed between the cost of the structure and its dimensions. Therefore, we also developed a third model of an artificial neural

network, which uses parameters 1-4, 6, the value of the outer diameter D_p in the range from D_{p2} to D_{p1} , and the ratio l/D_p . Based on seven input parameters, the third neural network determines the required pipe wall thickness t_p . A feedforward neural network with 2 hidden layers and 16 neurons on each layer was chosen as the ANN architecture. This architecture provided an optimal balance between the accuracy of the results and the cost of machine time for training. Single-layer models, as well as models with a smaller number of neurons, led to larger prediction errors. The architecture of the developed artificial neural networks is shown in Figs. (1 and 2). The activation function of the hidden layers neurons was taken as a hyperbolic tangent.

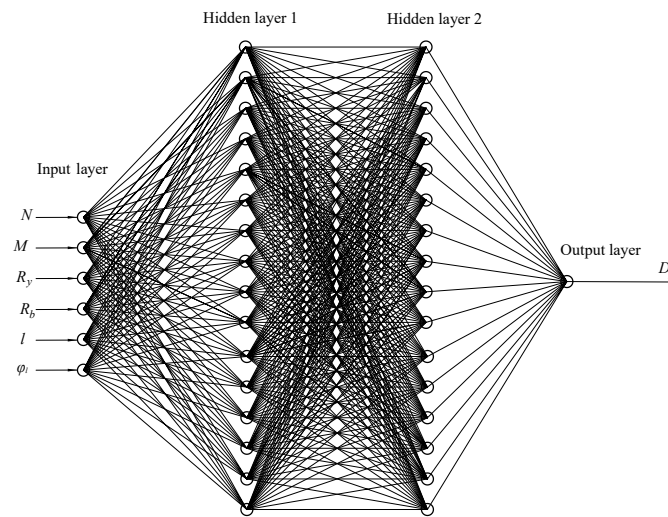


Fig. (1). Architecture of artificial neural networks for predicting the required column diameter.

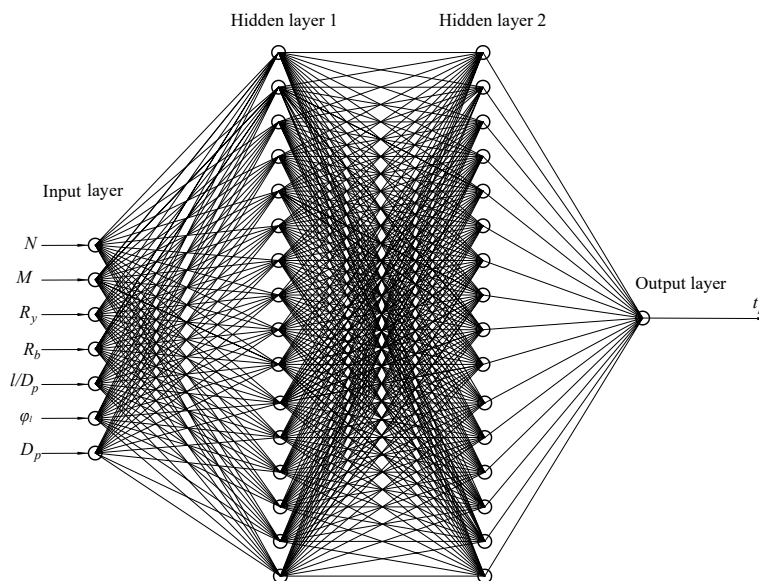


Fig. (2). Architecture of artificial neural network for predicting the required pipe wall thickness.

Table 1. Minimum and maximum wall thicknesses in accordance with GOST 10704-91.

No.	D_p , mm	Min t_p , mm	Max t_p , mm
1	102	1.8	5.5
2	108	1.8	5.5
3	114	1.8	5.5
4	127	1.8	5.5
5	133	1.8	5.5
6	140	1.8	5.5
7	152	1.8	5.5
8	159	1.8	8
9	168	1.8	8
10	177.8	1.8	8
11	180	4	5
12	193.7	2	8
13	219	2.5	22
14	244.5	3	22
15	273	3.5	22
16	325	4	22
17	355.6	4	22
18	377	4	22
19	406.4	4	22
20	426	4	22
21	478	5	12
22	508	4.5	24
23	530	5	20
24	630	7	24
25	720	7	30
26	820	7	30
27	920	7	20
28	1020	8	32
29	1120	8	20
30	1220	9	32
31	1420	10	32

The models were trained using synthetic data generated based on the provisions of Russian design codes for steel-reinforced concrete structures SR 266.1325.800.2016. Synthetic data were used because experimental data do not allow to cover the entire possible range of input parameters. Also, most of the experiments to determine the bearing capacity of CFST columns were performed on small-diameter samples. When forming training datasets, the value D_p varied from 102 to 1420 mm. The diameter values used in training the models, as well as the corresponding maximum and minimum wall thicknesses according to GOST 10704-91, are given in Table 1.

To ensure that the wall thickness is a non-decreasing function of the diameter, when forming the training dataset for model 1, the minimum thickness in row 11 was changed from 4 to 2 mm. For a similar purpose, when forming the training dataset for model 2, the maximum thickness in row 11 was changed from 5 to 8 mm, in row 21 from 12 to 22 mm, in row 23 from 20 to 24 mm, in row 27 from 20 to 30 mm, and in row 29 from 20 to 32 mm. The values that were adjusted are highlighted in bold in Table 1.

When forming training datasets for models 1 and 2, the value of concrete compressive strength R_b varied from 10 to 65 MPa with a step of 13.75 MPa (5 different values), the yield strength of steel R_y varied from 240 to 440 MPa with a step of 50 MPa (5 different values). The design column length l for each diameter value varied from $10 \cdot D_p$ up to $30 \cdot D_p$ in increments of $2 \cdot D_p$ (11 different values). The coefficient φ_l varied from 1 to 2 with a step of 0.2 (6 different values).

The ultimate bending moment for pure bending was determined according to SR266.1325800.2016 using the formula (Eq. 1):

$$M_{ult0} = \frac{2}{3} r_b^3 R_b \sin^3 \alpha + \frac{2}{\pi} A_p r_p \sin \alpha R_y, \quad (1)$$

where $r_b = (D_p - 2t_p) / 2$ is the radius of the concrete core, $r_p = (D_p - t_p) / 2$ is the radius of the middle surface of the pipe, $A_p = \pi D_p t_p$ and is the cross-sectional area of the steel pipe.

The angle α in Eq. 1 was determined from the solution of the equation (Eq. 2):

$$r_b^2 (\alpha - 0.5 \sin 2\alpha) R_{bp} + \frac{2\alpha}{\pi} A_p R_y - 1 = 0. \quad (2)$$

In addition to the ultimate bending moment, the ultimate axial force N_{ult0} under central compression was determined without taking into account random eccentricities and element slenderness using the formula (Eq. 3):

$$N_{ult0} = R_{pc} A_p + R_{bp} A_b, \quad (3)$$

where $R_{pc} = 0.75 R_y$ is the design strength of the pipe material under central compression, taking into account its operation in a biaxial stress state, $A_b = \pi \cdot 0.75 r_b^2$ is the area of the concrete core, R_{bp} is the design strength of the concrete taking into account the effect of lateral compression, determined under central compression using the formula (Eq. 4):

$$R_{bp} = R_b + \frac{2t_p}{D_p - 2t_p} R_y. \quad (4)$$

Next, the step for the bending moment was selected $\Delta M = M_{ult0} / (nM - 1)$, where nM is the number of calculated values of the bending moment. For each value of the bending moment M in the range from 0 to M_{ult0} with a step ΔM , the corresponding axial force at which the limit state occurs was calculated.

The determination of the ultimate axial force at a given bending moment was performed using a stepwise increase in the value of N from 0 to N_{ult0} in 1000 steps. The calculation was performed according to SR 266.1325800.2016 using the following algorithm:

1. At a given value M , the eccentricity of the axial force $e_0 = M/N$ was determined;

2. Additional random eccentricity e_a was calculated as the largest of three values (Eq. 5):

$$e_a = 1 \text{ cm}, e_a = D_p/30; e_a = l/600. \quad (5)$$

3. The coefficient η , taking into account the increase in eccentricity due to the deflection of the element, was determined using the formula (Eq. 6):

$$\eta = \frac{1}{1 - \frac{N}{N_{cr}}}, \quad (6)$$

where $N_{cr} = \pi^2 \cdot I^2 / l^2$ is the conditional critical force, D is reduced cross-sectional rigidity, determined by the formula (Eq. 7):

$$D = \min \begin{cases} k_b E_{b1} I + k_s E_s I_p; \\ k_b E_{b1} I + \frac{l^2}{\pi^2} \cdot 0.75 R_y A_p, \end{cases} \quad (7)$$

where $I = \pi \cdot \frac{(D_p - 2t_p)^4}{64}$ is the concrete core moment of

inertia, $I_p = \frac{\pi (D_p^4 - (D_p - 2t_p)^4)}{64}$ is the steel pipe moment of inertia, $E_s = 2.06 \cdot 10^5$ MPa is the steel modulus of elasticity, E_{b1} is the long-term concrete modulus of elasticity, determined by the formula (Eq. 8):

$$E_{b1} = \frac{E_{b0}}{1 + \varphi_{b,cr}}, \quad (8)$$

where E_{b0} is the concrete initial modulus of elasticity $\varphi_{b,cr}$ is the creep coefficient of concrete.

The initial concrete modulus of elasticity was determined based on the paper [30] as a function of its compressive strength using the formula (Eq. 9):

$$E_{b0} = 1000 \cdot \frac{0.05 R_b + 57}{1 + \frac{29}{3.8 + R_b}}, \text{ MPa} \quad (9)$$

Creep coefficient $\varphi_{b,cr}$ was determined using the empirical formula [31] (Eq. 10):

$$\varphi_{b,cr} = \frac{8000}{(E_{b0})^{0.785}}. \quad (10)$$

Coefficients k_s and k_b in Eq. 7 take into account the plastic work of concrete and steel pipe. The coefficient k_s is taken equal to 0.7, and the coefficient k_b is calculated using the formula (Eq. 11):

$$k_b = \frac{0.15}{\varphi_l (0.3 + \delta_e)}, \quad (11)$$

where $\delta_e = (e_0 + e_a) / D_p$ is the relative eccentricity of the axial force. At $\delta_e < 0.15$, the value 0.15 should be substituted into Eq. 11.

4. The calculated eccentricity of the axial force was determined (Eq. 12):

$$e = (e_0 + e_a) \cdot \eta \quad (12)$$

5. The design strength of concrete R_{bp} and steel pipe R_{pc} under compression as part of a reinforced concrete element was determined using the formulas (Eq. 13):

$$\begin{aligned} R_{bp} &= R_b + \Delta R_b \cdot m; \\ R_{pc} &= R_y - \frac{1}{4} R_y \cdot m, \end{aligned} \quad (13)$$

where

$$m = 1 - \frac{7.5e}{D_p - 2t_p} \geq 0, \Delta R_b = \left(2 + 2.52 e^{\frac{1}{c} (R_y A_p + R_b A_b)} \right) \frac{t_p}{D_p - 2t_p} R_y, c = 25 \text{ MN}.$$

6. The angle α , which determines the size of the compressed zone of concrete in the limit state, was calculated from the solution of the nonlinear equation (Eq. 14):

$$r_b^2 (\alpha - 0.5 \sin(2\alpha)) R_{bp} + \frac{\alpha}{\pi} A_p R_{pc} - \left(1 - \frac{\alpha}{\pi} \right) A_p R_y - N = 0. \quad (14)$$

7. The ultimate bending moment M_{ult} was determined using the formula (Eq. 15):

$$M_{ult} = \frac{2}{3} r_b^3 R_{bp} \sin^3 \alpha + \frac{1}{\pi} A_p r_p \sin \alpha (R_y + R_{pc}); \quad (15)$$

When the product $N \cdot e$ exceeds the value M_{ult} at the current load step, then the value N is taken as the ultimate value and written to the training dataset as an input

parameter. The current value of the column D_p diameter is written to the training dataset as an output parameter. The number of calculated values of the bending moment nM when forming the training datasets for the first and second models was taken to be 41. Thus, the total volume of the training datasets for the first and second models was $31 \cdot 5 \cdot 5 \cdot 41 \cdot 11 \cdot 6 = 2097150$ numerical experiments. Fragments of the generated data for models 1 and 2 are given in Tables 2 and 3.

Table 2. Fragment of the generated dataset for model 1, predicting the column diameter with a minimum pipe wall thickness.

No.	N , kN	M , kN · m	R_y , MPa	R_b , MPa	l , m	φ_i	Dp_i , mm
1	116.66	0.00	240	10	1.02	1	102
2	113.70	0.12	240	10	1.02	1	102
3	110.99	0.25	240	10	1.02	1	102
4	108.28	0.37	240	10	1.02	1	102
5	105.56	0.49	240	10	1.02	1	102
6	102.36	0.62	240	10	1.02	1	102
7	99.15	0.74	240	10	1.02	1	102
8	95.94	0.87	240	10	1.02	1	102
9	92.49	0.99	240	10	1.02	1	102
10	89.28	1.11	240	10	1.02	1	102
...
2097141	2613.60	9176.55	440	65	42.6	2	1420
2097142	2364.69	9472.57	440	65	42.6	2	1420
2097143	2115.77	9768.59	440	65	42.6	2	1420
2097144	1866.86	10064.61	440	65	42.6	2	1420
2097145	1493.49	10360.62	440	65	42.6	2	1420
2097146	1244.57	10656.64	440	65	42.6	2	1420
2097147	995.66	10952.66	440	65	42.6	2	1420
2097148	622.29	11248.68	440	65	42.6	2	1420
2097149	373.37	11544.70	440	65	42.6	2	1420
2097150	0.00	11840.71	440	65	42.6	2	1420

Table 3. Fragment of the generated dataset for model 2, predicting the column diameter at maximum pipe wall thickness.

No.	N , kN	M , kN · m	R_y , MPa	R_b , MPa	l , m	φ_i	Dp_i , mm
1	262.64	0.00	240	10	1.02	1	102
2	255.79	0.34	240	10	1.02	1	102
3	248.37	0.68	240	10	1.02	1	102
4	241.52	1.02	240	10	1.02	1	102
5	234.66	1.35	240	10	1.02	1	102
6	227.24	1.69	240	10	1.02	1	102
7	219.82	2.03	240	10	1.02	1	102
8	212.97	2.37	240	10	1.02	1	102
9	206.12	2.71	240	10	1.02	1	102
10	199.27	3.05	240	10	1.02	1	102
...
2097141	6838.73	26092.78	440	65	42.6	2	1420
2097142	6154.86	26934.48	440	65	42.6	2	1420
2097143	5470.99	27776.18	440	65	42.6	2	1420
2097144	4787.11	28617.89	440	65	42.6	2	1420
2097145	3932.27	29459.59	440	65	42.6	2	1420

(Table 3) contd....

No.	N, kN	M, kN • m	R_y , MPa	R_b , MPa	l, m	φ_i	D_{p2} , mm
2097146	3248.40	30301.29	440	65	42.6	2	1420
2097147	2393.56	31142.99	440	65	42.6	2	1420
2097148	1709.68	31984.70	440	65	42.6	2	1420
2097149	854.84	32826.40	440	65	42.6	2	1420
2097150	0.00	33668.10	440	65	42.6	2	1420

Table 4. Fragment of the training dataset for model 3, predicting the required wall thickness for a given diameter D_p [D_{p2} ; D_{p1}].

No.	N, kN	M, kN • m	R_y , MPa	R_b , MPa	$\frac{l}{D_p}$	φ_i	D_p , mm	t_p , mm
1	116.66	0.00	240	10	10	1	102	1.8
2	105.56	0.49	240	10	10	1	102	1.8
3	92.49	0.99	240	10	10	1	102	1.8
4	79.91	1.48	240	10	10	1	102	1.8
5	67.83	1.98	240	10	10	1	102	1.8
6	55.99	2.47	240	10	10	1	102	1.8
7	44.64	2.97	240	10	10	1	102	1.8
8	33.30	3.46	240	10	10	1	102	1.8
9	22.20	3.96	240	10	10	1	102	1.8
10	11.35	4.45	240	10	10	1	102	1.8
...
2045991	24961.37	3366.81	440	65	30	2	1420	32
2045992	22225.88	6733.62	440	65	30	2	1420	32
2045993	19661.35	10100.43	440	65	30	2	1420	32
2045994	16925.86	13467.24	440	65	30	2	1420	32
2045995	14361.34	16834.05	440	65	30	2	1420	32
2045996	11796.81	20200.86	440	65	30	2	1420	32
2045997	9061.32	23567.67	440	65	30	2	1420	32
2045998	6154.86	26934.48	440	65	30	2	1420	32
2045999	3248.40	30301.29	440	65	30	2	1420	32
2046000	0.00	33668.10	440	65	30	2	1420	32

When forming the training dataset for the third model predicting the required wall thickness, Table 1 was used in its original form without adjustments. The range of input parameters was the same as for models 1 and 2. Since the third model contained one more parameter than models 1 and 2, the number of calculated values for the parameter φ_i was reduced to 5, and the number of calculated values of the bending moment was reduced to 11. The parameter l/D_p varied from 10 to 30 with a step of 4 (6 different values). The wall thickness for each diameter in the assortment varied from $t_{p,min}$ to $t_{p,max}$ with a step

$$\frac{t_{p,max} - t_{p,min}}{7}$$

(8 different values). The total volume of the training dataset for model 3 was $31 \cdot 5 \cdot 5 \cdot 11 \cdot 6 \cdot 5 \cdot 8 = 2046000$ numerical experiments. A fragment of the training dataset for model 3 is given in Table 4.

Artificial neural network models were implemented in the MATLAB environment. During training, the generated

datasets were randomly divided into three parts: "Train", "Validation" and "Test" in the proportion of 70%: 15%: 15%. The mean squared error (MSE) value was adopted as a metric of training quality. Minimization of the MSE value was performed using the Levenberg-Marquardt optimization algorithm. This algorithm was chosen because it allows achieving the lowest neural network error, often with the lowest time costs [32]. The algorithm provides an acceptable compromise between the convergence rate inherent in Newton algorithms and the stability inherent in the gradient descent algorithm [33]. The number of iterations in the training process for all models was taken to be 1000 (**Supplementary dataset 1-3**).

3. RESULTS AND DISCUSSION

Figs. (3-5) shows the training performance graphs for models 1-3. Trained models are characterized by low mean squared error values, which are 8.96 mm^2 for model 1, 7.3 mm^2 for model 2 and 0.03 mm^2 for model 3.

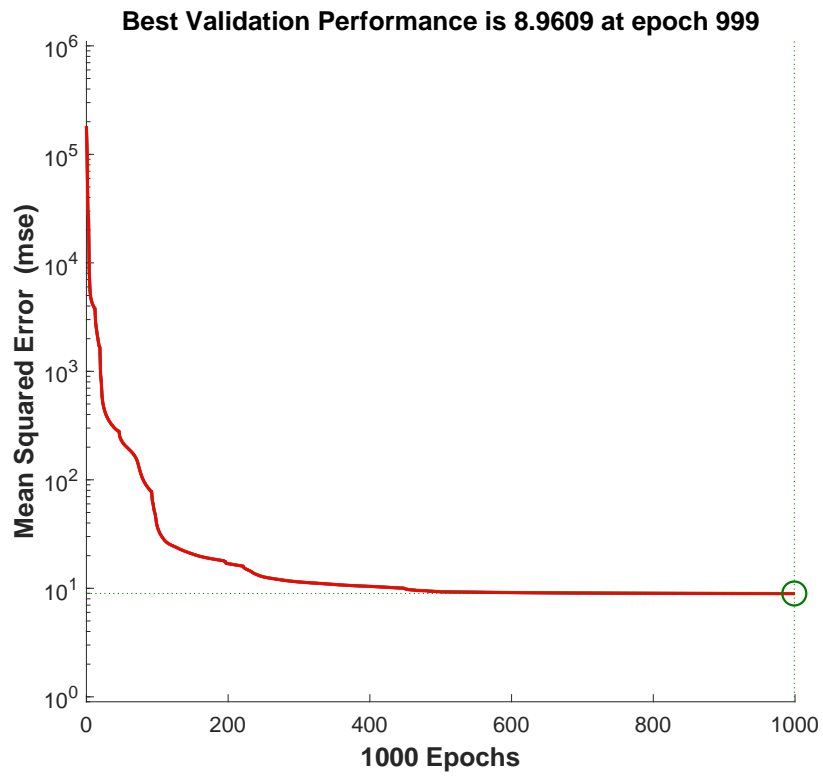


Fig. (3). Training performance graph for model 1.

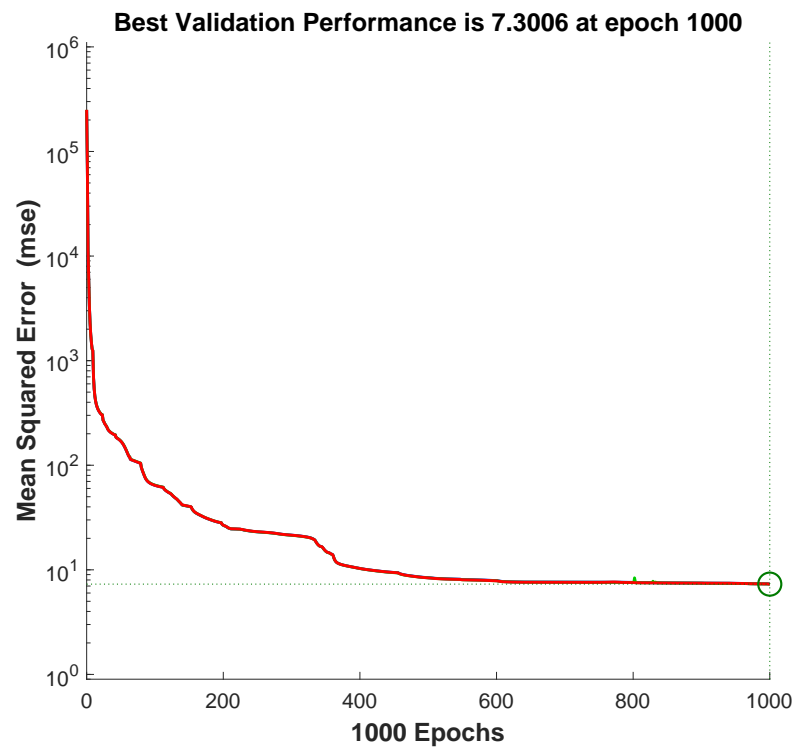


Fig. (4). Training performance graph for model 2.

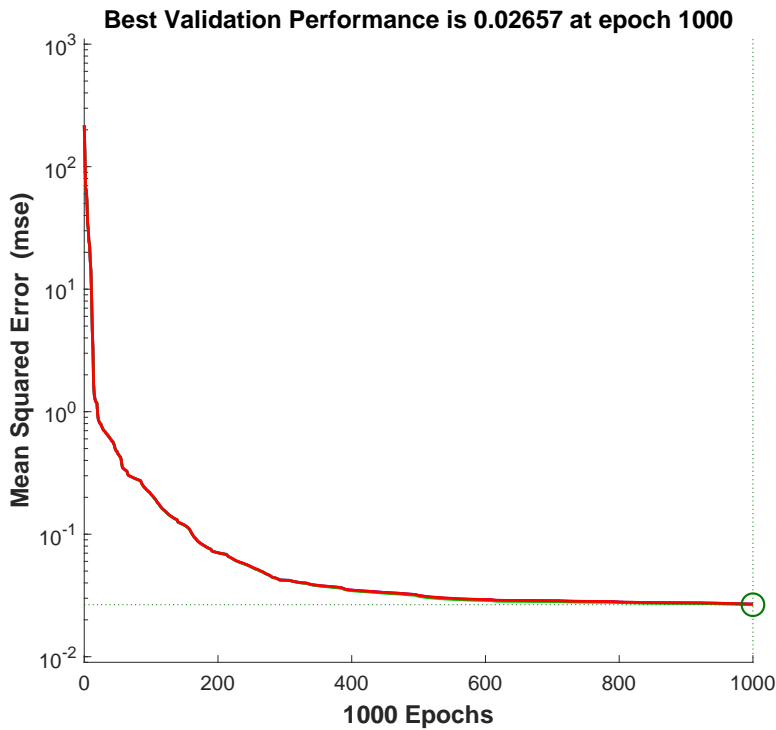


Fig. (5). Training performance graph for model 3.

Figs. (6 and 7) show the regression plots for models 1-2. The target values T of the column diameters are plotted along the abscissa axis, and the values Y predicted by the neural network are plotted along the ordinate axis.

All points on the graphs lie at a slight distance from the straight line $Y = T$. The correlation coefficients R between the target and predicted values differ slightly from $R = 1$ for the “Train”, “Validation”, and “Test” samples, as well as for the entire dataset as a whole.

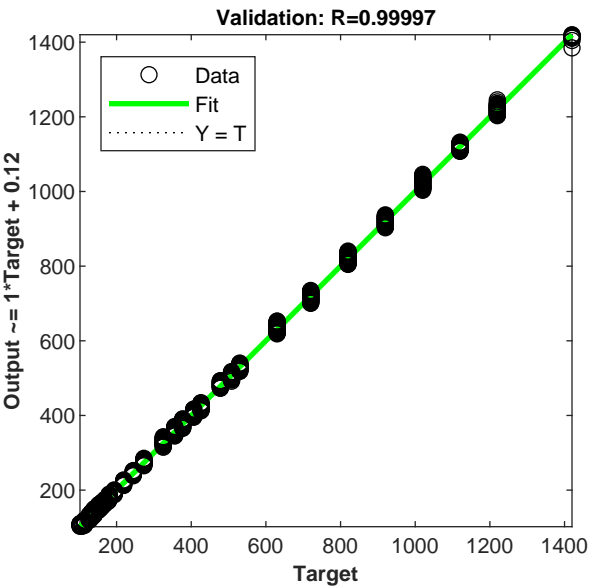
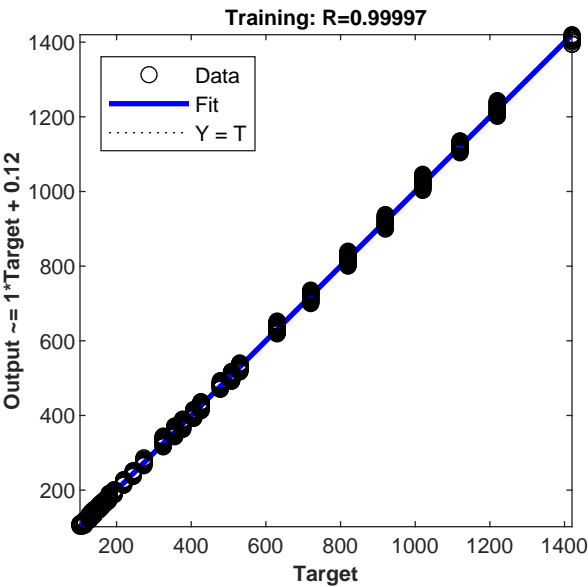


Fig. 6 contd.....

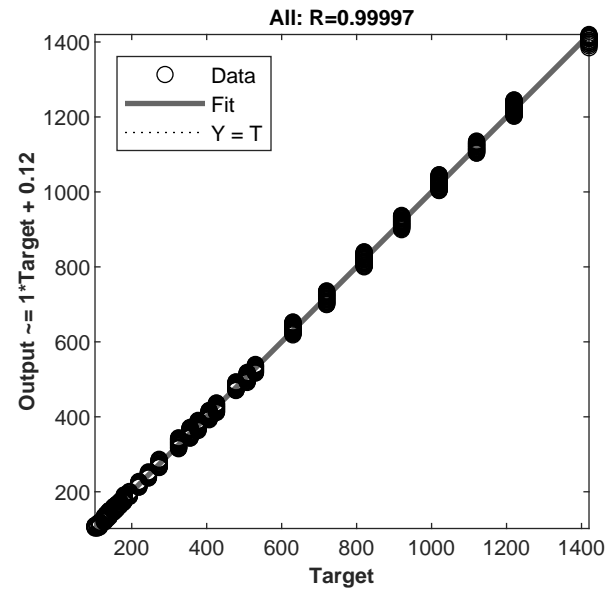
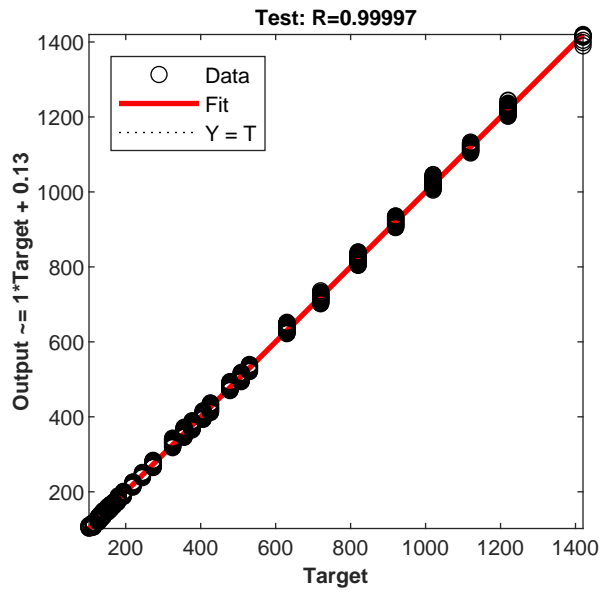


Fig. (6). Regression plots for model 1.

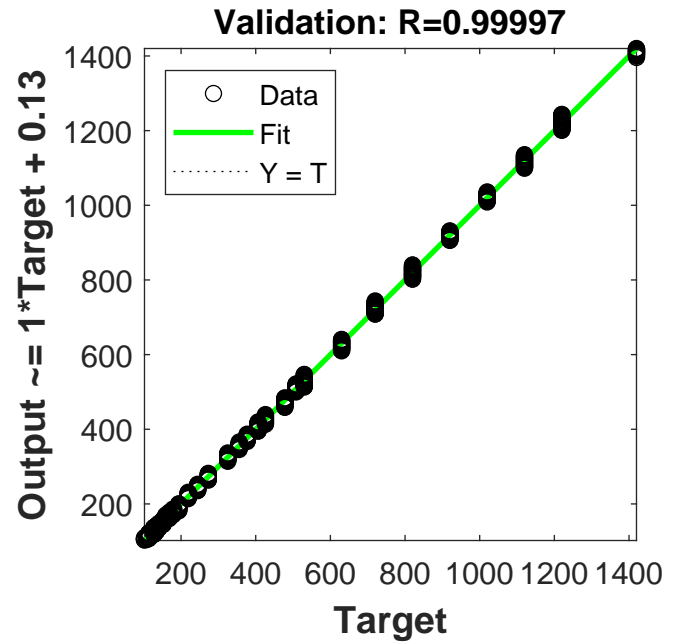
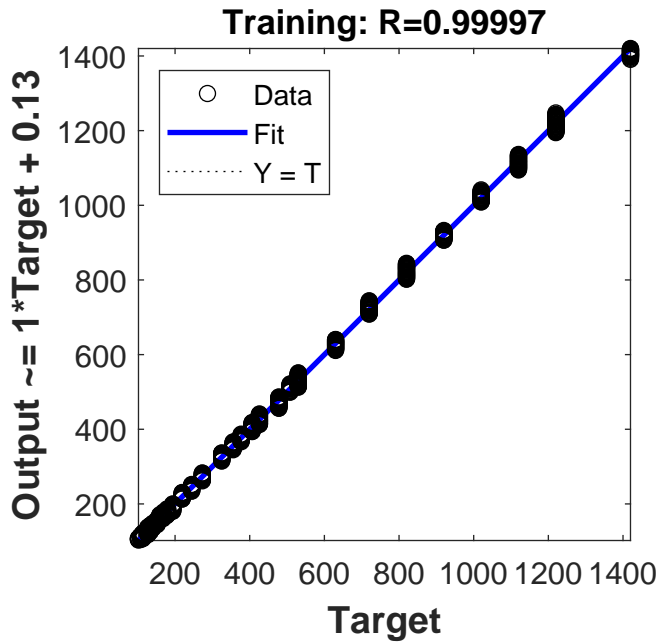


Fig. 7 contd....

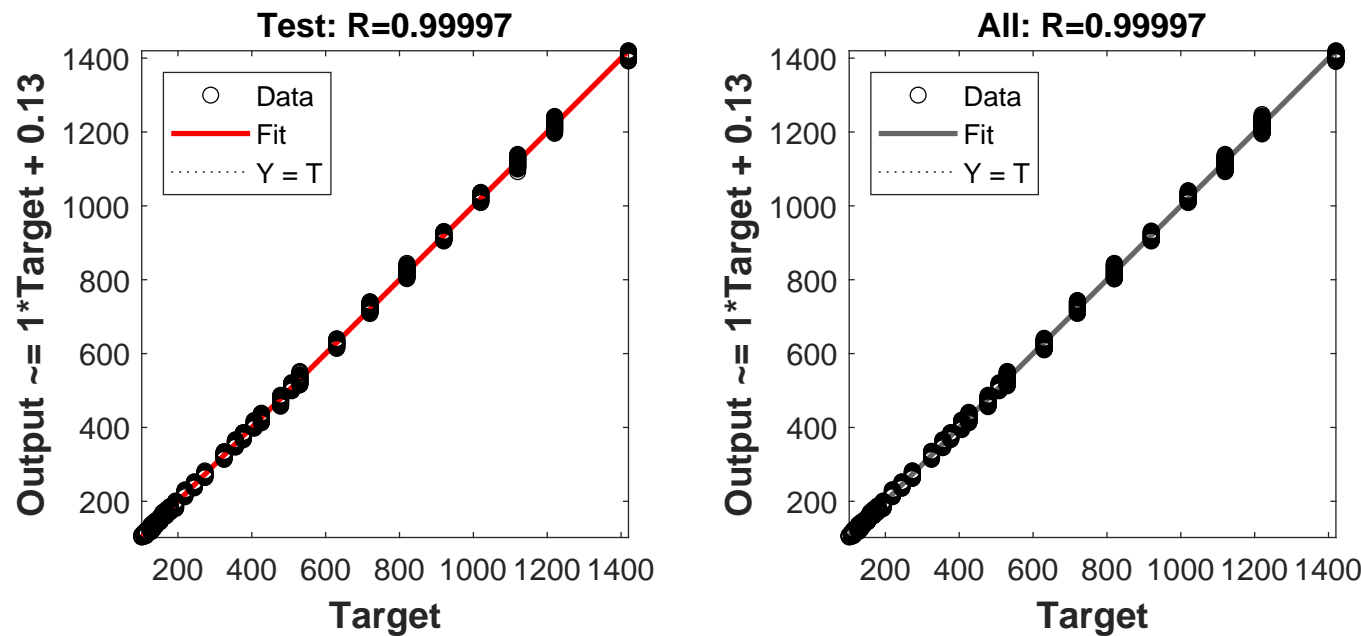


Fig. (7). Regression plots for model 2.

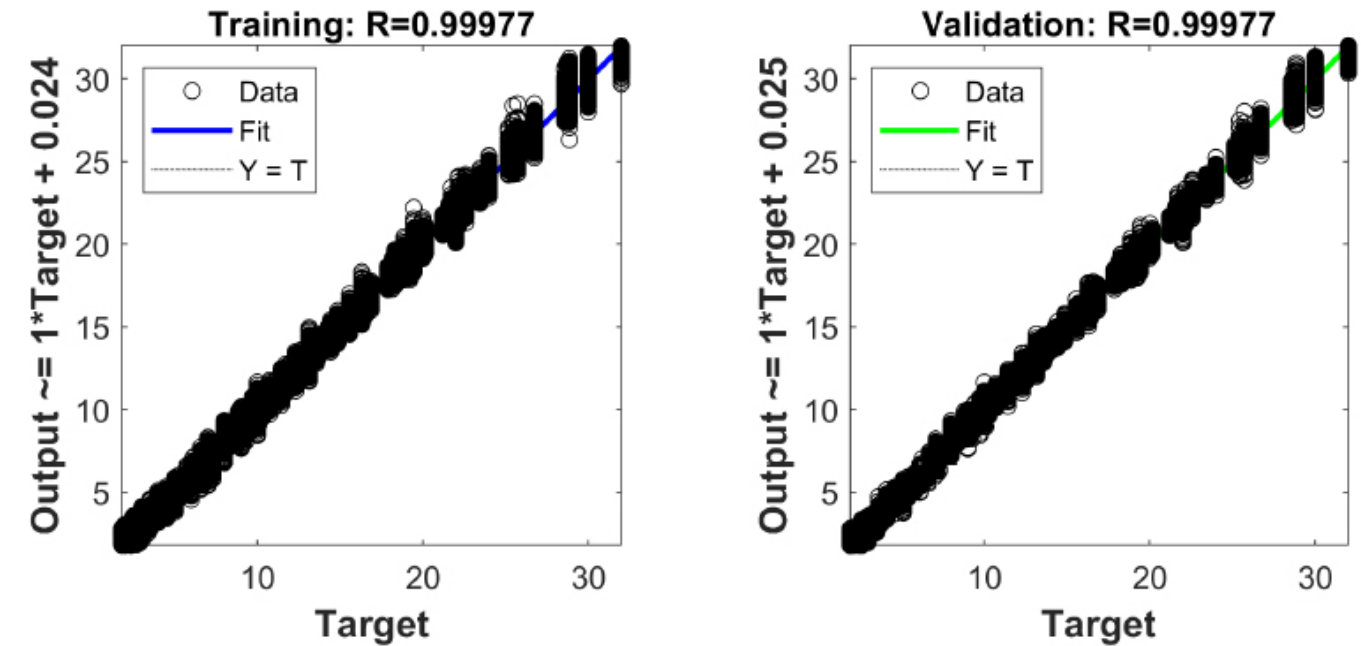


Fig. 8 contd.....

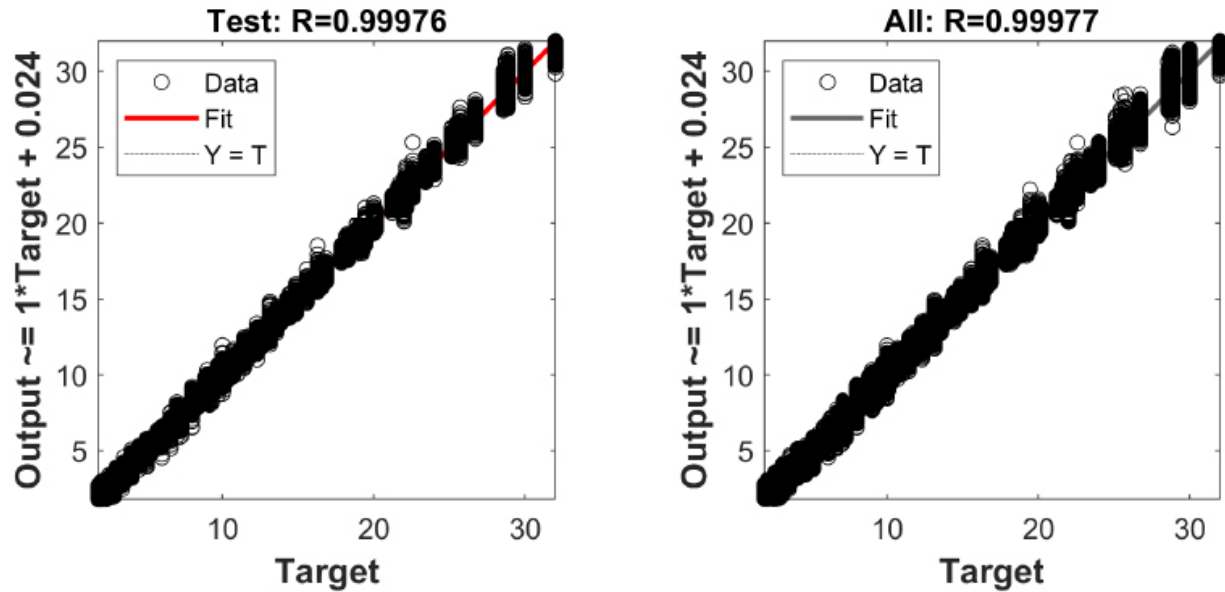


Fig. (8). Regression plots for model 3.

Table 5. Feature importance for models 1 and 2.

		Input parameter					
		N	M	R_y	R_b	l	φ_i
Importance, %	Model 1	58.6	128.39	4.77	3.03	33.78	0.99
	Model 2	51.44	118.1	6.41	2.02	100.17	0.29

Table 6. Feature importance for model 3.

	Input Parameter						
	N	M	R_y	R_b	l/D_p	φ_i	D_p
Importance, %	338.41	385.26	15.36	7.48	9.19	2.06	59.35

Fig. (8) shows the regression plots for model 3, predicting the required pipe wall thickness. In contrast to Figs. (6 and 7), the scatter of data relative to the straight line $Y = T$ is more pronounced. This can be explained by the fact that model 3 includes one more input parameter than models 1 and 2, with approximately the same volume of the training dataset. Nevertheless, the correlation coefficients between the target and predicted wall thickness values are also close to 1. In the practical application of model 3, the engineer should round off the wall thickness value predicted by the model to the nearest one according to the assortment.

Thus, the developed artificial neural network models can act as a reliable and effective tool for determining the required cross-sectional size of eccentrically compressed CFST columns.

Machine learning methods, including artificial neural networks, also allow us to evaluate the importance of

features. We chose the method of fixing values as a method for evaluating the feature's importance. The essence of this method is to calculate the relative difference between the value at the output of the neural network with a fixed value of the feature and the value at the output determined with a full set of features. As a fixed value of the feature, its average value for the entire sample is selected.

Table 5 shows the importance of the input parameters in percentage for models 1 and 2. This table shows that the values of internal forces and the design length of the element exert the greatest influence on the required value of the column diameter. The strength characteristics of steel and concrete have a lesser influence on the cross-sectional dimensions, and the influence of the coefficient φ_i is the most insignificant.

Table 6 shows the importance of the input parameters for model 3. Here, the least influence of the parameter φ_i

on the pipe wall thickness is also observed. The parameters that most significantly influence the required pipe wall thickness include the values of internal forces, as well as the outer diameter of the column.

Feature importance analysis allows civil engineers to identify those parameters that can be ignored during analysis in the first approximation. In our case, this is the φ_l coefficient, which characterizes the share of long-term loads in the total load on the column.

CONCLUSION

Three models of artificial neural networks have been developed to predict the cross-sectional dimensions of eccentrically compressed CFST columns. The first model, based on the magnitude of internal forces, material characteristics, design length, and data on the share of long-term loads in the total load, predicts what cross-sectional diameter is required with a minimum pipe wall thickness according to the assortment of electric-welded straight-seam pipes. The second model predicts the required diameter with the maximum possible wall thickness. Having a possible range of column diameter variation, the third machine-learning model can then determine what wall thickness is required for any diameter from the obtained range. The developed models have shown high prediction efficiency based on MSE indicators and the correlation coefficient between target and predicted values. The reliability of the results is ensured by the large size of the training datasets, which included more than 2 million samples. The proposed models can be integrated into the form of utilities into existing software packages for designing building structures (CivilFEM, LIRA-SAPR, SCAD, etc.)

The importance of the features was also assessed using the variable fixation method. It was found that the required column diameter is most significantly affected by the values of internal forces and its design length. The strength characteristics of concrete and steel have a lesser effect on the cross-sectional dimensions. The required wall thickness of a steel pipe is most significantly affected by the value of the axial force and bending moment, as well as the cross-sectional diameter.

In this paper, only CFST columns with a circular cross-section were considered. However, at large eccentricities of axial forces, columns with a rectangular cross-section work more effectively on eccentric compression [34-36]. The prospect of further research may be the development of machine learning models for selecting the cross-sectional dimensions of rectangular CFST columns.

AUTHORS' CONTRIBUTIONS

V.T. conceived and designed the study. A.C. and V.A. collected the data. S.A.Z. drafted the manuscript. All authors reviewed the results and approved the final version of the manuscript.

LIST OF ABBREVIATIONS

ANN	=	Artificial Neural Networks
CFST	=	Concrete-filled Steel Tubular

AI	=	Artificial Intelligence
ML	=	Machine Learning
GEP	=	Genetic Programming
GA	=	Genetic Algorithm
SVR	=	Support Vector Regression
SR	=	Symbolic Regression
MSE	=	Mean Squared Error

CONSENT FOR PUBLICATION

Not applicable.

AVAILABILITY OF DATA AND MATERIAL

The data supporting the findings of the article is available in the Yandex Disk at <https://disk.yandex.ru/d/p-5RKsDcXwTWBQ>

FUNDING

None.

CONFLICT OF INTEREST

The authors declare no conflict of interest. The funders had no role in the design of the study; in the collection, analyses, or interpretation of data; in the writing of the manuscript; or in the decision to publish the results.

ACKNOWLEDGEMENTS

The authors would like to acknowledge the administration of Don State Technical University, Russia for their resources and financial support.

SUPPLEMENTARY MATERIAL

Supplementary material is available on the publisher's website along with the published article.

REFERENCES

- [1] L. Ma, H. Wang, and J. Zhang, "Axial compression experiment and numerical simulation of CFST short columns at an ultra early age", *Structures*, vol. 59, p. 105674, 2024.
[<http://dx.doi.org/10.1016/j.istruc.2023.105674>]
- [2] C. Yang, P. Gao, X. Wu, Y.F. Chen, Q. Li, and Z. Li, "Practical formula for predicting axial strength of circular-CFST columns considering size effect", *J. Construct. Steel Res.*, vol. 168, p. 105979, 2020.
[<http://dx.doi.org/10.1016/j.jcsr.2020.105979>]
- [3] J.H. Wang, J. He, and Y. Xiao, "Fire behavior and performance of concrete-filled steel tubular columns: Review and discussion", *J. Construct. Steel Res.*, vol. 157, pp. 19-31, 2019.
[<http://dx.doi.org/10.1016/j.jcsr.2019.02.012>]
- [4] K. Chung, S. Park, and S. Choi, "Material effect for predicting the fire resistance of concrete-filled square steel tube column under constant axial load", *J. Construct. Steel Res.*, vol. 64, no. 12, pp. 1505-1515, 2008.
[<http://dx.doi.org/10.1016/j.jcsr.2008.01.002>]
- [5] A.L. Krishan, V.I. Rimshin, and M.A. Astafieva, "Strength of centrally compressed tube-concrete nlms of improved design", *Construction. Reconstruction*, vol. 3, no. 77, pp. 12-21, 2018.
- [6] A.L. Krishan, V.I. Rimshin, and E.A. Troshkina, "Strength of short concrete filled steel tube columns of annular cross section", *IOP Conf. Ser.: Mater. Sci. Eng.*, vol. 463, no. 2, p. 022062, 2018.
[<http://dx.doi.org/10.1088/1757-899X/463/2/022062>]

- [7] M.L. Romero, A. Espinós, A. Lapuebla-Ferri, V. Alberro, and A. Hospitaler, "Recent developments and fire design provisions for CFST columns and slim-floor beams", *J. Construct. Steel Res.*, vol. 172, p. 106159, 2020.
[<http://dx.doi.org/10.1016/j.jcsr.2020.106159>]
- [8] L.H. Han, C.Y. Xu, and Z. Tao, "Performance of concrete filled stainless steel tubular (CFSST) columns and joints: Summary of recent research", *J. Construct. Steel Res.*, vol. 152, pp. 117-131, 2019.
[<http://dx.doi.org/10.1016/j.jcsr.2018.02.038>]
- [9] K. Kloppel, and W. Goder, "Load tests with concrete-lined steel pipes and establishment of a design formula", *Steel construction.*, vol. 26, no. 1, pp. 1-10, 1957.
- [10] C.D. Goode, and D. Lam, "Concrete - filled steel tube columns - tests compared with Eurocode 4", In: *Composite Construction in Steel and Concrete VI*, American Society of Civil Engineers, 2011, pp. 317-325..
- [11] M. Denavit, "Steel-concrete composite column database", Available from: <https://mark.denavit.me/Composite-Column-Database/>
- [12] Z. Tao, U.Y. Brian, L.H. Han, and S.H. He, "Design of concrete-filled steel tubular members according to the Australian Standard AS 5100 model and calibration", *Australian J. Struct. Eng.*, vol. 8, no. 3, pp. 197-214, 2008.
[<http://dx.doi.org/10.1080/13287982.2008.11464998>]
- [13] R. Leon, T. Perea, J. Hajjar, and M. Denavit, "Concrete-filled tubes columns and beam-columns: A database for the AISC 2005 and 2010 specifications", Available from: <https://coe.northeastern.edu/research/compositeframes/papers/Leon%20et%20al%202011%20-%20Festschrift%20Gerhard%20Hanswille.pdf>
- [14] J. Hajjar, *Steel-concrete composite structural systems.*, Dept. of Civil and Environmental Engineering, Northeastern Univ.: Boston, 2013.
- [15] J.Y.R. Liew, M. Xiong, and D. Xiong, "Design of concrete filled tubular beam-columns with high strength steel and concrete", *Structures*, vol. 8, pp. 213-226, 2016.
[<http://dx.doi.org/10.1016/j.istruc.2016.05.005>]
- [16] K. Kourou, T.P. Exarchos, K.P. Exarchos, M.V. Karamouzis, and D.I. Fotiadis, "Machine learning applications in cancer prognosis and prediction", *Comput. Struct. Biotechnol. J.*, vol. 13, pp. 8-17, 2015.
[<http://dx.doi.org/10.1016/j.csbj.2014.11.005>] [PMID: 25750696]
- [17] M. Ahmadi, H. Naderpour, and A. Kheyroddin, "Utilization of artificial neural networks to prediction of the capacity of CCFT short columns subject to short term axial load", *Arch. Civ. Mech. Eng.*, vol. 14, no. 3, pp. 510-517, 2014.
[<http://dx.doi.org/10.1016/j.acme.2014.01.006>]
- [18] M. Ahmadi, H. Naderpour, and A. Kheyroddin, "ANN model for predicting the compressive strength of circular steel-confined concrete", *Int. J. Civ. Eng.*, vol. 15, no. 2, pp. 213-221, 2017.
[<http://dx.doi.org/10.1007/s40999-016-0096-0>]
- [19] Y. Du, Z. Chen, C. Zhang, and X. Cao, "Research on axial bearing capacity of rectangular concrete-filled steel tubular columns based on artificial neural networks", *Front. Comput. Sci.*, vol. 11, no. 5, pp. 863-873, 2017.
[<http://dx.doi.org/10.1007/s11704-016-5113-6>]
- [20] T.T. Le, P.G. Asteris, and M.E. Lemonis, "Prediction of axial load capacity of rectangular concrete-filled steel tube columns using machine learning techniques", *Eng. Comput.*, vol. 38, no. S4, pp. 3283-3316, 2022.
[<http://dx.doi.org/10.1007/s00366-021-01461-0>]
- [21] V.-L. Tran, and S.-E. Kim, "A new empirical formula for prediction of the axial compression capacity of CCFT columns", *Steel Compos. Struct.*, vol. 33, pp. 181-194, 2019.
[<http://dx.doi.org/10.12989/scs.2019.33.2.181>]
- [22] V.L. Tran, D.K. Thai, and S.E. Kim, "Application of ANN in predicting ACC of SCFST column", *Compos. Struct.*, vol. 228, p. 111332, 2019.
[<http://dx.doi.org/10.1016/j.compstruct.2019.111332>]
- [23] V.L. Tran, D.K. Thai, and D.D. Nguyen, "Practical artificial neural network tool for predicting the axial compression capacity of circular concrete-filled steel tube columns with ultra-high-strength concrete", *Thin-walled Struct.*, vol. 151, p. 106720, 2020.
[<http://dx.doi.org/10.1016/j.tws.2020.106720>]
- [24] E.M. Güneyisi, A. Gültekin, and K. Mermerdaş, "Ultimate capacity prediction of axially loaded CFST short columns", *Int. J. Steel Struct.*, vol. 16, no. 1, pp. 99-114, 2016.
[<http://dx.doi.org/10.1007/s13296-016-3009-9>]
- [25] M.F. Javed, F. Farooq, S.A. Memon, A. Akbar, M.A. Khan, F. Aslam, R. Alyousef, H. Alabduljabbar, and S.K.U. Rehman, "New prediction model for the ultimate axial capacity of concrete-filled steel tubes: An evolutionary approach", *Crystals*, vol. 10, no. 9, p. 741, 2020.
[<http://dx.doi.org/10.3390/cryst10090741>]
- [26] M.Z. Naser, S. Thai, and H.-T. Thai, "Evaluating structural response of concrete-filled steel tubular columns through machine learning", *J. Build. Eng.*, vol. 34, p. 101888, 2021.
[<http://dx.doi.org/10.1016/j.jobe.2020.101888>]
- [27] A. Memarzadeh, H. Sabetifar, and M. Nematzadeh, "A comprehensive and reliable investigation of axial capacity of Sy-CFST columns using machine learning-based models", *Eng. Struct.*, vol. 284, no. January, p. 115956, 2023.
[<http://dx.doi.org/10.1016/j.engstruct.2023.115956>]
- [28] K. Megahed, N.S. Mahmoud, and S.E.M. Abd-Rabou, "Application of machine learning models in the capacity prediction of RCFST columns", *Sci. Rep.*, vol. 13, no. 1, p. 20878, 2023.
[<http://dx.doi.org/10.1038/s41598-023-48044-1>] [PMID: 38012229]
- [29] I. Faridmehr, M.L. Nehdi, A.F. Nejad, M.A. Sahraei, H. Kamyab, and K.A. Valerievich, "An innovative multi-objective optimization approach for compact concrete-filled steel tubular (CFST) column design utilizing lightweight high-strength concrete", *Int. J. Lightweight. Material. Manufacture*, vol. 7, no. 3, pp. 405-425, 2024.
[<http://dx.doi.org/10.1016/j.ijlmm.2024.01.004>]
- [30] G. Nesvetaev, Y. Koryanova, and B. Yazyev, "Autogenous shrinkage and early cracking of massive foundation slabs", *Magazine. Civil Eng.*, vol. 17, no. 6, pp. 1-3, 2024.
[<http://dx.doi.org/10.34910/MCE.130.5>]
- [31] G.V. Nesvetaev, Y.I. Koryanova, and V.V. Shut, "Specific heat dissipation of concrete and the risk of early cracking of massive reinforced concrete foundation slabs", *Construction Material. Products*, vol. 7, no. 4, p. 3, 2024.
[<http://dx.doi.org/10.58224/2618-7183-2024-7-4-3>]
- [32] S. Sapna, A. Tamilarasi, and M.P. Kumar, "Backpropagation learning algorithm based on Levenberg Marquardt Algorithm", *Comput. Sci. Inf. Technol.*, vol. 2, pp. 393-398, 2012. [CS and IT].
[<http://dx.doi.org/10.5121/csit.2012.2438>]
- [33] I. Mukherjee, and S. Routroy, "Comparing the performance of neural networks developed by using Levenberg-Marquardt and Quasi-Newton with the gradient descent algorithm for modelling a multiple response grinding process", *Expert Syst. Appl.*, vol. 39, no. 3, pp. 2397-2407, 2012.
[<http://dx.doi.org/10.1016/j.eswa.2011.08.087>]
- [34] Y.F. Yang, F. Fu, and X.M. Bie, "Behaviour of rectangular RACFST slender columns under eccentric compression", *J. Build. Eng.*, vol. 38, p. 102236, 2021.
- [35] P. Du, Y.X. Ma, and K.H. Tan, "Experimental study of ultra-high-performance fibre-reinforced concrete (UHPFRC)-encased CFST short columns under axial and eccentric compression", *Eng. Struct.*, vol. 316, p. 118452, 2024.
[<http://dx.doi.org/10.1016/j.engstruct.2024.118452>]
- [36] A. Raza, A. Selmi, M. Hechmi El Ouni, N. Ghazouani, and B. Ahmed, "Reliability analysis of normal strength CFST rectangular columns through multiple approaches", *Expert Syst. Appl.*, vol. 255, p. 124901, 2024.
[<http://dx.doi.org/10.1016/j.eswa.2024.124901>]